ELSEVIER

23 October 1995

PHYSICS LETTERS A

Physics Letters A 207 (1995) 93–104

# Stochastic resonance and optimal design of threshold detectors

P. Jung

*Department of Physics and Center for Complex Systems Research, Beckman Institute, University of Illinois, Urbana, IL 61801, USA*

Received 16 June 1995; accepted for publication 8 August 1995
Communicated by C.R. Doering

**Abstract**

We consider the detection of noisy signals with neuron-like threshold crossing detectors in the context of stochastic resonance. On the basis of an exact spectral analysis of the outgoing stochastic spike train, we show for the first time that there are optimal values for the threshold which yield under given environmental conditions optimal performance.

## 1. Introduction

Threshold crossing dynamics appears to be very common in nature and technology. Nowadays communication technology e.g. relies almost exclusively on digital information processing, where analog–digital converters are of vital importance. The human brain manages its outstanding information processing capability by relying on action potentials of its numerous neurons.

In a very idealized description, threshold systems perform some action whenever some voltage or other input quantity exceeds a given threshold. As common as the occurrence of threshold crossing dynamics is the presence of noise, coming with the input signal or being inherent in the threshold devices. The typical noise level, however, can vary over a large range. In electronic communication systems, the noise level is typically very small, whereas in neuronal systems the noise amplitude can easily be as large as that of the information carrying signals. It is the purpose of this paper to study the impact of noise on the performance of threshold devices and to provide optimal design strategies at given environmental conditions.

The threshold system we are studying responds with an action (pulse $h(t)$) when the noisy input exceeds a threshold (see also Refs. [1,2]). The pulse is completely uncorrelated with the time evolution of the input. The output of the threshold system is a train of pulses $h(t)$ located each at the times $t_n$ where the input crosses threshold, i.e.

$$s(t) = \sum_n h(t - t_n) = \int \mathrm{d}t'\, s_\delta(t - t')h(t'),$$

$$s_\delta(t) = \sum_n \delta(t - t_n). \qquad (1)$$

Since the statistical properties of the pulse train are contained in the sequence of "random points" $t_n$, it is sufficient to study $s_\delta(t)$. The pulse-shape $h(t)$ yields for e.g. the power spectrum of the pulse-train only a multiplicative form factor.

As the input of our device, we consider a sinusoidal signal contaminated by Gaussian colored noise. For weak signal amplitudes, the stochastic spike train (1) has been studied recently in Ref. [2] by simulating the threshold crossing dynamics and analyzing the spectral properties of the pulse train (see also Ref. [3] for a review). It has turned out that the signal-to-noise ra-


*SSDI* 0375-9601(95)00636-2

tio (SNR) of the pulse train assumes a maximum at a finite noise level – a novel form of stochastic resonance [4] (for recent reviews see Refs. [5,6]).

Two theoretical approaches to describe this novel form of stochastic resonance have been developed recently. Wiesenfeld et al. [1] have analyzed the coherence of the spike train by computing the signal-to-noise ratio, based on the assumption that the spikes are statistically independent and that the signal amplitude is small against the threshold. Another approximative treatment has been put forward by Gingl, Kiss and Moss [2] by taking advantage of the assumption of a slow input signal (low frequency) and small signal amplitudes.

In order to find conditions for optimal performance of threshold detectors, it is necessary to overcome the restrictions of the previous theoretical results. In Sections 1–6, we derive from scratch exact expressions for the statistical and spectral properties of the random pulse train generated by the threshold device, driven by a sinusoidal signal and Gaussian colored noise. The exact results are compared with the approximate theories mentioned above. In particular, we calculate spike–spike correlation functions and discuss their impact on the power spectrum of the pulse train. Having results at hand which are not restricted in parameter space, we discuss the optimal design of threshold detectors in Section 7. Given the input and the environmental conditions of the threshold detector, i.e. the signal strength, noise level and signal-to-noise ratio, we determine the design-parameter (threshold value) which yields the highest signal intensity or the highest signal-to-noise ratio.

## 2. Threshold crossing rates

In this section we consider the threshold crossing statistics of the sum $x(t)$ of a sinusoidal signal $A\sin(\Omega t)$ and colored Gaussian noise $\xi(t)$. In order that the threshold-crossing rates are finite, the spectral density of the noise has to decay with at least the inverse fourth power of the frequency [7]. Applying Gaussian white noise to a second order low-pass filter yields Gaussian colored noise with the required property, i.e.

$$\ddot{\xi} + \left(\frac{1}{\tau_1} + \frac{1}{\tau_2}\right)\dot{\xi} + \frac{1}{\tau_1\tau_2}\xi(t) = \frac{\sqrt{D}}{\tau_1\tau_2}\Gamma(t),$$
$$\langle \Gamma(t)\Gamma(t')\rangle = 2\delta(t-t'), \tag{2}$$

where $\tau_1$ and $\tau_2$ are filter constants. A linear transformation to the sum $x(t) = \xi(t) + A\sin(\Omega t)$ and its derivative $v(t) = \dot{\xi} + \Omega\cos(\Omega t)$, yields an Ornstein–Uhlenbeck process with a drift term which is periodic in time. The transition probability density for this pair process is known explicitly [5] (see also Section 5). Denoting by $t_n$ the times when the sum $x(t)$ crosses the threshold $b$ from below, the number of threshold crossings in the interval $[0,t]$ is given by

$$n(t) = \int_0^t \sum_n \delta(t'-t_n)\,\mathrm{d}t'$$
$$= \int_0^t \Theta(v(t'))v(t')\delta(x(t')-b)\,\mathrm{d}t'. \tag{3}$$

The average number of crossings per time interval (threshold crossing rate) is obtained from Eq. (3) by taking the ensemble average or equivalently by averaging the last term in Eq. (3) over the probability density $P(x,v,t)$. For a stationary process $(x,v)$ (e.g. in the absence of the signal $A\sin(\Omega t)$), the stationary threshold crossing rate is obtained by averaging over the stationary probability density

$$P_{\mathrm{st}}(x,v) = \frac{1}{2\pi\sqrt{\sigma^2\sigma_v^2}}\exp\left(-\frac{x^2}{2\sigma^2} - \frac{v^2}{2\sigma_v^2}\right), \tag{4}$$

with

$$\sigma^2 = \frac{D}{\tau_1+\tau_2}, \quad \sigma_v^2 = \frac{D}{\tau_1\tau_2(\tau_1+\tau_2)}, \tag{5}$$

yielding [7]

$$r_{\mathrm{cr}}(A=0) = \langle \dot{n}(t)\rangle = \int_0^\infty v P_{\mathrm{st}}(b,v)\,\mathrm{d}v$$
$$= \frac{1}{2\pi\sqrt{\tau_1\tau_2}}\exp(-b^2/2\sigma^2). \tag{6}$$

In the presence of the signal ($A \neq 0$), the inhomogeneous threshold crossing rate is given by

$$r_{\rm cr}(t) = \langle \dot{n}(t) \rangle = \int_0^\infty {\rm d}v\, v P_{\rm as}(x = b, v, t), \tag{7}$$

with $P_{\rm as}(x, v, t)$ being the long time asymptotic probability density of the pair process $(x(t), v(t))$ [8,5],

$$P_{\rm as}(x, v, t) = \frac{1}{2\pi\sqrt{\sigma^2 \sigma_v^2}} \exp\left( - \frac{[x - A\sin(\Omega t)]^2}{2\sigma^2} - \frac{[v - A\Omega\cos(\Omega t)]^2}{2\sigma_v^2} \right). \tag{8}$$

Inserting (8) into (7) one obtains for the inhomogeneous threshold crossing rate

$$\begin{aligned} r_{\rm cr}(t) &\equiv \langle \dot{n} \rangle \\ &= \frac{1}{2\pi\sqrt{\tau_1 \tau_2}} \exp\left( - \frac{[1 - \bar{A}\sin(\Omega t)]^2}{2\bar{\sigma}^2} \right) \\ &\times \left[ \exp\left( - \frac{A^2}{2\bar{\sigma}^2} \right) + \tfrac{1}{2}\bar{A}\epsilon \sqrt{\frac{2\pi}{\bar{\sigma}^2}} \right. \\ &\left. \times \cos(\Omega t) {\rm erfc}\left( - \frac{\bar{A}\epsilon\cos(\Omega t)}{\sqrt{2\bar{\sigma}^2}} \right) \right], \end{aligned} \tag{9}$$

with the dimensionless scaled parameters

$$\bar{A} = A/b, \quad \bar{\sigma}^2 = \sigma^2/b^2, \quad \epsilon = \sqrt{\Omega^2 \tau_1 \tau_2}. \tag{10}$$

In the adiabatic limit $\Omega \to 0$, i.e. $\epsilon \to 0$, we obtain an expression of the type obtained in Ref. [2]. It is important to note that the second term in (9) becomes large for large signal amplitudes $A$ even if the frequency $\Omega$ is small. Neglecting this term therefore implies besides the adiabatic condition a limitation to small signal amplitudes.

## 3. The power spectrum of the spike train

As the next step we calculate the spectral properties of the $\delta$-spike train, generated by the above described statistical threshold process. If the crossing times $t_n$ would be independent (white shot noise), the spectral density of the spike train will be frequency independent [7]. For the model we are looking at, we do not know a priori whether the correlations between the spikes are negligible, and therefore have to calculate the power-spectrum from scratch. The stochastic $\delta$-pulse train ($h(t) = s_0\delta(t)$), generated by the threshold device is written as

$$\begin{aligned} s(t) &= s_0 \dot{n}(t) = s_0 \sum_n \delta(t - t_n) \\ &= s_0 \Theta(v) v \delta(x(t) - b). \end{aligned} \tag{11}$$

Using the generalized Wiener–Khintchin theorem for periodically driven stochastic processes [5], the spectral density of the spike train is given by the Fourier transform of the time-averaged correlation function

$$\begin{aligned} K_{\rm av}(\tau) &= \frac{1}{T} \int_0^T K_2(t' + \tau, t')\, {\rm d}t', \\ K_2(t, t') &= s_0^2 \langle \dot{n}(t) \dot{n}(t') \rangle. \end{aligned} \tag{12}$$

Inserting Eq. (11) into Eq. (12) one finds for the correlation function (see also Appendix A)

$$\begin{aligned} K_2(t, t') = s_0^2 \int_0^\infty {\rm d}v \int_0^\infty {\rm d}v'\, v v' P(b, v, t | b, v', t') \\ \times P_{\rm as}(b, v', t'), \end{aligned} \tag{13}$$

where $P(x, v, t | x, v', t')$ is the conditional probability density, which is known explicitly for the threshold model under consideration (see Ref. [8] and Section 5). As can be seen from Eq. (13), the correlation function has a singularity at $t = t'$. We can split this singularity off the correlation function by using results from the theory of random points (see Appendix A), i.e.

$$K_2(t, t') = s_0^2 r_{\rm cr}(t) \delta(t - t') + s_0^2 f_2(t, t'), \tag{14}$$

where $f_2(t, t')$ is a smooth function at $t = t'$. The meaning of $f_2(t, t')$ becomes clear when we subtract the long-time limit of the correlation function $K_2(t \gg t') = f_2(t \gg t') \to r_{\rm cr}(t) r_{\rm cr}(t')$. Then, the contribution additional to the $\delta$-correlation is the spike–spike correlation function

$$g_2(t, t') = f_2(t, t') - r_{\rm cr}(t) r_{\rm cr}(t') \tag{15}$$

(see Ref. [7] and Appendix A).

Using Eq. (14), the time averaged correlation function $K_{\rm av}(\tau)$ (12) can be written as the sum of a $\delta$-contribution and a smooth correlation function, i.e.

$$K_{\rm av}(\tau) = s_0^2 \langle r_{\rm cr}(t) \rangle_t \delta(\tau) + s_0^2 f_{\rm av}(\tau),$$

$$f_{\rm av}(\tau) = \frac{1}{T}\int_0^T f_2(t'+\tau, t')\,{\rm d}t', \tag{16}$$

with $\langle r_{\rm cr}(t)\rangle_t$ being the time averaged threshold crossing rate. The spectral density consists of the sum of a constant (white shot noise) and a frequency dependent part, i.e.

$$S(\omega) = s_0^2\langle r_{\rm cr}\rangle_t + s_0^2 S_f(\omega),$$

$$S_f(\omega) = \int_{-\infty}^{\infty} {\rm e}^{-{\rm i}\omega\tau} f_{\rm av}(\tau)\,{\rm d}\tau. \tag{17}$$

## 4. Signal intensity

As already mentioned above, the correlation function $K_2(t,t')$ decays for a large time difference $t$ into the product of the time inhomogeneous threshold crossing rates $r_{\rm cr}(t)r_{\rm cr}(t')$. Performing the time average over the time $t'$ according to Eq. (12), we observe that the time averaged correlation function (in the large time limit) is periodic in time. Expanding the inhomogeneous threshold crossing ratc (9) into a Fourier series, we find for the time averaged smooth correlation function for large times (i.e. $f_{\rm av}(\tau) = K_{\rm av}(\tau)$),

$$f_{\rm av}(\tau) = \sum_{n=-\infty}^{\infty} |c_n|^2\,{\rm e}^{{\rm i}n\Omega\tau},$$

$$c_n = \frac{1}{T}\int_0^T r_{\rm cr}(\tau)\,{\rm e}^{-{\rm i}n\Omega\tau}\,{\rm d}\tau, \tag{18}$$

and subsequently the sum of $\delta$-spikes for the power spectrum

$$S_\delta(\omega) = s_0^2\int_{-\infty}^{\infty} f_{\rm av}(\tau)\,{\rm e}^{-{\rm i}\omega\tau}\,{\rm d}\tau$$

$$= 2\pi s_0^2\sum_{n=-\infty}^{\infty} |c_n|^2\delta(\omega - n\Omega). \tag{19}$$

The Fourier coefficients $c_n$ have to be computed numerically from Eqs. (9) and (18). The non-periodic decaying part of the spike–spike correlation function adds a broad noise-background to the spectral density; the $\delta$-spikes and their intensities, however, remain unchanged. The intensity $4\pi s_0^2|c_n|^2$ of the $\delta$-spikes at the frequency $\Omega$, i.e. the intensity of the output signal, describe how deep the periodic input signal is actually coded in the spike train. In Fig. 1, the signal intensity normalized by $s_0^2$ is shown as a function of the variance of the noise $\bar\sigma^2$ and the signal amplitude $\bar A$.

For sub-threshold signals, i.e. $\bar A < 1$, the intensity of the spike vanishes for vanishing noise. For increasing noise, we find an increasing spike intensity, i.e. the signal is coded by the threshold element although the amplitude of the input signal is smaller than the threshold. The reason for this behavior is the synchronization of the random threshold crossings by the external signal. When the noise becomes too large, the threshold crossing gets out of synchronization with the signal and the signal intensity decreases again. This phenomenon has been discussed in Refs. [2,1,9] for weak input signals as a novel form of stochastic resonance.

For signals above threshold, the signal intensity approaches for vanishing noise its finite deterministic value, given by

$$4\pi s_0^2|c_1|^2 = 4\pi s_0^2|\langle\delta(A\sin(\Omega t) - b)\,{\rm e}^{-{\rm i}\Omega t}\rangle|^2$$

$$= s_0^2\frac{\Omega^2}{\pi}\Theta(\bar A - 1) = \frac{\epsilon^2 s_0^2}{\pi\tau_1\tau_2}\Theta(\bar A - 1), \tag{20}$$

with the Heaviside step function, defined by $\Theta(x > 0) = 1$ and $\Theta(x < 0) = 0$. For increasing $\bar A$, the intensity of the signal increases until it reaches a maximum and then increases again. The reason for this behavior is the following: Once the input signal has crossed the threshold the element cannot fire unless the input signal first re-crosses the threshold from above to below. Therefore, there is independent of the signal amplitude exactly one crossing within each period in the absence of noise. In the presence of noise, additional spikes occur most likely when the input signal $A\sin(\Omega t)$ is in the vicinity of the threshold. The noise induced increase of the spiking activity – similar to that for sub-threshold signals – is therefore synchronized with the external signal, yielding a resonance-like curve as a function of the noise strength.

The form of stochastic resonance observed here is unusual for two reasons. First, the dependence of the peak position on the signal frequency is very weak [2,9], i.e. the peak does not move towards zero noise

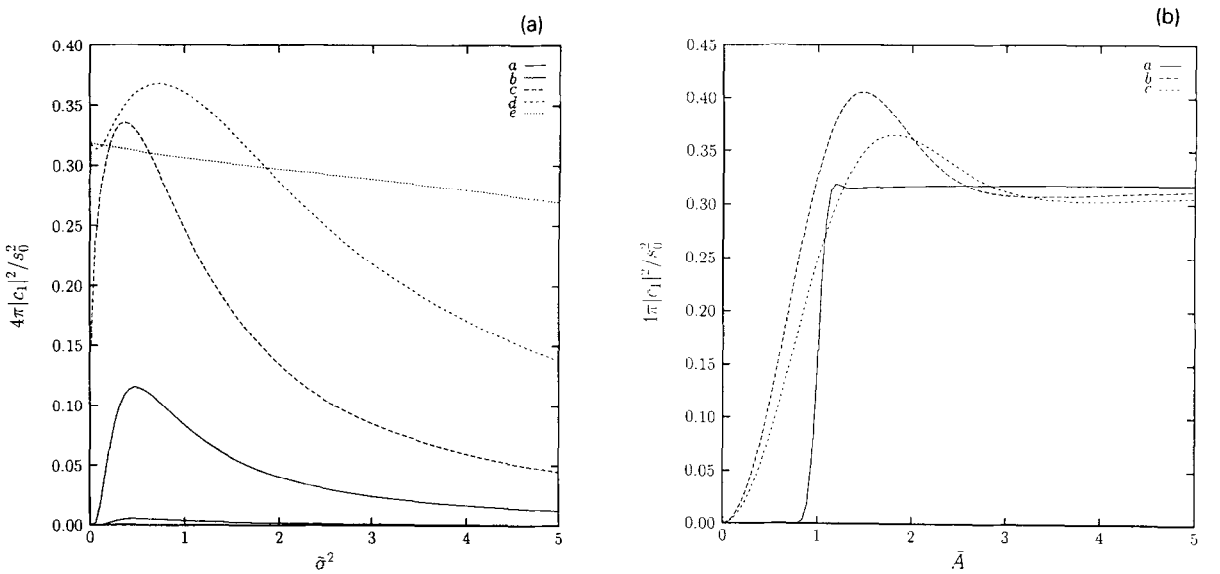


Fig. 1. (a) Signal intensity as a function of the variance of the noise for $\bar{A} = 0.1$ (a), $\bar{A} = 0.5$ (b), $\bar{A} = 1$ (c), $\bar{A} = 2$ (d) and $\bar{A} = 5$ (d) at $\tau_1 = 0.9, \tau_2 = 0.1$ and $\epsilon = \sqrt{\Omega^2\tau_1\tau_2} = 0.3$. (b) Signal intensity as a function of the amplitude $\bar{A}$ for $\sigma^2 = 0.01$ (a), $\sigma^2 = 0.5$ (b) and $\sigma^2 = 1$ (c) at $\tau_1 = 0.9, \tau_2 = 0.1$ and $\epsilon = \sqrt{\Omega^2\tau_1\tau_2} = 0.3$.

as the frequency $\Omega$ approaches zero. Second, we observe stochastic resonance also for excitations *above* threshold.

As a function of the signal amplitude $\bar{A}$, we also find non-monotonic behavior, since once the amplitude of the input signal is well above threshold, the time intervals where additional noise induced spikes occur decrease with increasing $\bar{A}$. The limit of infinite signal amplitude is again the deterministic limit obtained (20) in the absence of the noise for an arbitrary super-threshold signal.

For weak signals $\bar{A} \ll 1$, the Fourier coefficient $c_n$ can be computed analytically, yielding for the intensity of the spike in the power spectrum of the spike train at $\Omega$,

$$4\pi s_0^2|c_1|^2 = \tfrac{1}{2}\bar{A}^2 s_0^2 r_0^2\left(\frac{1}{\bar{\sigma}^4} + \epsilon^2\frac{\pi}{2\bar{\sigma}^2}\right). \tag{21}$$

The first term on the r.h.s. of (21), i.e. the adiabatic limit, is analogous to the results in Refs. [2] and [1]. The second term introduces a dependence on the signal frequency $\Omega$, which moves the peak position from $\bar{\sigma}^2 = b^2/2$ for $\epsilon = 0$ to larger values of the noise level as the driving frequency increases. It also provides the leading order term for large noise. The decrease of the signal intensity for increasing large noise is proportional to $1/\sigma^2$ as opposed to $1/\sigma^4$ in the adiabatic limit ($\epsilon = 0$). The latter effect might be the explanation for the disagreement of neuronal data with the approximations for large noise intensities in Ref. [1].

## 5. Spike–spike correlation functions

The time averaged spike–spike correlation function

$$g_{\mathrm{av}}(\tau) = f_{\mathrm{av}}(\tau) - \frac{1}{T}\int_0^T r_{\mathrm{cr}}(t')r_{\mathrm{cr}}(t'+\tau)$$

$$= f_{\mathrm{av}}(\tau) - \sum_{n=-\infty}^{\infty}|c_n|^2\,\mathrm{e}^{\mathrm{i}n\Omega t}, \tag{22}$$

with $f_{\mathrm{av}}(\tau)$ related to $K_{\mathrm{av}}(\tau)$ in (16) can be obtained for our model up to quadratures. Using the asymptotic probability density (8) and the transition probability density [5]

$$P(x,v,t|x',v',t') = \frac{1}{2\pi\sqrt{\det(\boldsymbol{\sigma})}} \times \exp[-\alpha(t)(x-x_t)^2]\exp[-\beta(t)(v-v_t)^2] \times \exp[-\gamma(t)(x-x_t)(v-v_t)], \quad (23)$$

with

$$x_t(x',v',t') = C_1\exp\left(-\frac{t-t'}{\tau_1}\right) + C_2\exp\left(-\frac{t-t'}{\tau_2}\right) + A\sin(\Omega t),$$

$$v_t(x',v',t') = -\frac{C_1}{\tau_1}\exp\left(-\frac{t-t'}{\tau_1}\right) - \frac{C_2}{\tau_2}\exp\left(-\frac{t-t'}{\tau_2}\right) + A\Omega\cos(\Omega t),$$

$$C_1 = \frac{\tau_1\tau_2}{\tau_1-\tau_2} \times \left(v' + \frac{1}{\tau_2}[x' - A\sin(\Omega t') - A\Omega\cos(\Omega t')]\right),$$

$$C_2 = \frac{\tau_1\tau_2}{\tau_2-\tau_1} \times \left(v' + \frac{1}{\tau_1}[x' - A\sin(\Omega t') - A\Omega\cos(\Omega t')]\right) - A\sin(\Omega t'), \quad (24)$$

and

$$\alpha(t) = \frac{1}{2}\frac{\sigma_v^2(t)}{\det(\boldsymbol{\sigma})}, \quad \beta(t) = \frac{1}{2}\frac{\sigma^2(t)}{\det(\boldsymbol{\sigma})},$$

$$\gamma(t) = -\frac{\sigma_{xv}(t)}{\det(\boldsymbol{\sigma})}, \quad \det(\boldsymbol{\sigma}) = \sigma^2(t)\sigma_v^2(t) - \sigma_{xv}^2(t),$$

$$\sigma^2(t) = \frac{D}{(\tau_1-\tau_2)^2}\left(\tau_1+\tau_2 + \frac{4\tau_1\tau_2}{\tau_1+\tau_2}\left\{\exp\left[-\left(\frac{1}{\tau_1}+\frac{1}{\tau_2}\right)t\right]-1\right\} - \tau_1\exp\left(-\frac{2t}{\tau_1}\right) - \tau_2\exp\left(-\frac{2t}{\tau_2}\right)\right),$$

$$\sigma_v^2(t) = \frac{D}{(\tau_1-\tau_2)^2}\left(\frac{1}{\tau_1}+\frac{1}{\tau_2} + \frac{4}{\tau_1+\tau_2}\left\{\exp\left[-\left(\frac{1}{\tau_1}+\frac{1}{\tau_2}\right)t\right]-1\right\} - \frac{1}{\tau_1}\exp\left(-\frac{2t}{\tau_1}\right) - \frac{1}{\tau_2}\exp\left(-\frac{2t}{\tau_2}\right)\right),$$

$$\sigma_{xv}(t) = \frac{D}{(\tau_1-\tau_2)^2}\left[\exp\left(-\frac{t}{\tau_1}\right) - \exp\left(-\frac{t}{\tau_2}\right)\right]^2. \quad (25)$$

One of the integrations in (13) can be carried out, yielding

$$K_2(t,t') = \frac{1}{4\pi^2\sqrt{\sigma^2\sigma_v^2\det(\boldsymbol{\sigma})}}\int_0^\infty dv'\, v' \times \exp\left(-\frac{1}{2\sigma(t)}[b - x_t(b,v',t')]^2\right)V(t,t'),$$

$$V(t,t') = \frac{1}{2\beta(t)}\exp[-\beta(t)\delta^2(t,t')] + \frac{1}{2}\sqrt{\frac{\pi}{\beta(t)}}\delta(t,t')\operatorname{erfc}(\sqrt{\beta(t)\delta^2(t,t')}),$$

$$\delta(t,t') = v_t - \frac{\gamma(t)}{2\beta(t)}(b - x_t), \quad (26)$$

with the variances $\sigma$ and $\sigma_v$ of the asymptotic probability density $P_{as}(x,v,t)$ given in Eq. (5). The integration in (26) and the subsequent time averages to obtain $g_{av}(\tau)$ have to be carried out numerically.

For a Poissonian process $g_{av}(\tau)$ as well as all higher order point-correlation functions are zero. The quantity $g_{av}(\tau)$ is therefore a good measure of how much the spiking of the threshold element deviates from that of a Poissonian process.

The spike–spike correlation function $g_{av}(\tau)$ is shown for $\bar{A} = 0$ and $\bar{A} = 0.5$, $\Omega = 1$ for various values of the strength of the fluctuations in Fig. 2a and Fig. 2b, respectively. For weak noise, the amplitude of the spike–spike correlation function is relatively small and decays monotonically in time, since spiking is a rare event and the stochastic process driving the threshold system is almost Markovian on the time-scale of a typical inter-spike time-interval. For larger noise, the spike–spike correlations function first increase, reach a maximum and then decay to zero. The *dip* of the correlations at small times is the consequence of a build-in refractory behavior – a sort of spike-repulsion. The stochastic process driving the threshold system has a smooth first derivative since it is *twice* low-pass filtered white noise. The larger the time scales $\tau_1$ and $\tau_2$ (i.e. the smaller the cut-off frequency), the smoother the process. Having crossed the threshold, say at time $t$, the smoothness of the

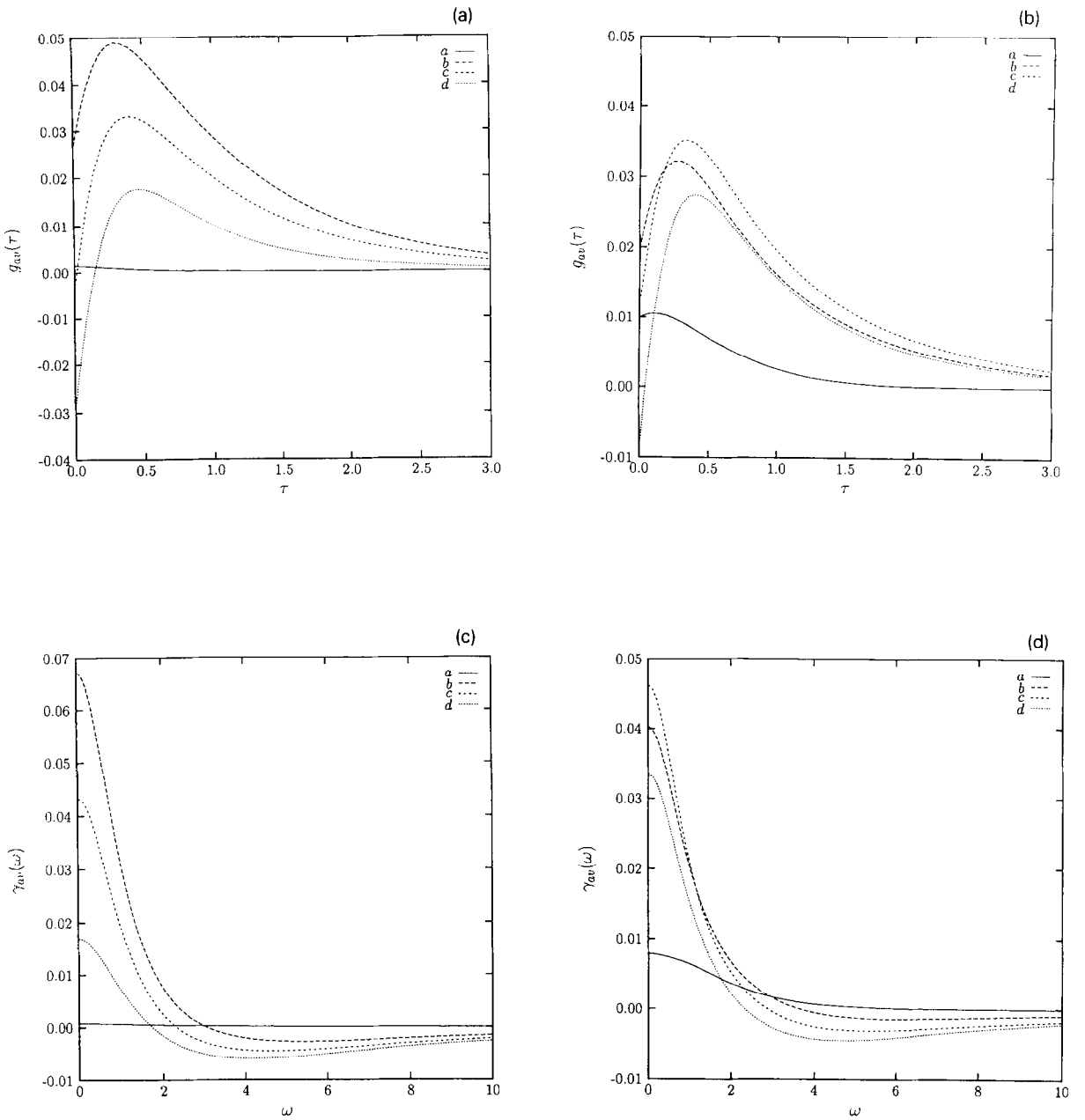


Fig. 2. (a) Spike–spike correlation function in the absence of a periodic input signal ($\bar{A} = 0$) for $\sigma^2 = 0.1$ (a), $\sigma^2 = 1$ (b), $\sigma^2 = 2$ (c) and $\sigma^2 = 4$ (d) at $\tau_1 = 0.9, \tau_2 = 0.1$. (b) The spike–spike correlation function at $\bar{A} = 0.5$ for $\sigma^2 = 0.1$ (a), $\sigma^2 = 0.5$ (b), $\sigma^2 = 1$ (c) and $\sigma^2 = 2$ (d) at $\tau_1 = 0.9, \tau_2 = 0.1$ and $\epsilon = \sqrt{\Omega^2 \tau_1 \tau_2} = 0.3$. (c) Fourier transform of the spike–spike correlation function at $\bar{A} = 0$ for $\sigma^2 = 0.1$ (a), $\sigma^2 = 1$ (b), $\sigma^2 = 2$ (c) and $\sigma^2 = 4$ (d) at $\tau_1 = 0.9, \tau_2 = 0.1$. (d) Fourier transform of the spike–spike correlation function at $\bar{A} = 0.5$ for $\sigma^2 = 0.1$ (a), $\sigma^2 = 1$ (b), $\sigma^2 = 2$ (c) and $\sigma^2 = 4$ (d) at $\tau_1 = 0.9, \tau_2 = 0.1$ and $\epsilon = \sqrt{\Omega^2 \tau_1 \tau_2} = 0.3$.

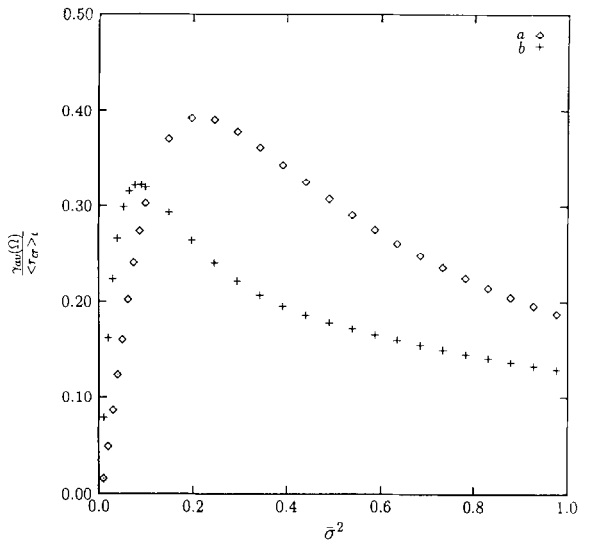


Fig. 3. Ratio of the contribution of the spike–spike correlation function and the white shot noise to the spectral density as a function of the noise level for $\bar{A} = 0$ (a) and $\bar{A} = 0.5$ (b) at $\tau_1 = 0.9, \tau_2 = 0.1$ and $\epsilon = \sqrt{\Omega^2 \tau_1 \tau_2} = 0.3$ (b).

process requires a certain amount of time to recross the threshold – the refractory time. Within this time-interval a threshold crossing event is unlikely. This explanation is supported by the observation that the position of the maximum moves to larger times for larger $\tau_1$ and $\tau_2$ and vice versa.

The Fourier transform $\gamma_{av}(\omega)$ of the time averaged spike–spike correlation function $g_{av}(\tau)$, a smooth function which decays to zero for large frequencies, describes the deviation from a frequency-independent shot-noise spectrum (see Figs. 2c, 2d).

The impact of the spike–spike correlation function on the spectral density is shown by plotting the ratio of $\gamma_{av}(\Omega)$ and the spectral density of the shot noise $\langle r_{cr}(t) \rangle_t = c_0$ as a function of the variance of the noise $\sigma$ in Fig. 3.

For the parameters chosen here, i.e. $\tau_1 = 0.9, \tau_2 = 0.1$, the contribution of the spike–spike correlations to the noise background is smaller than the shot-noise contribution $\langle r_{cr}(t) \rangle_t$. For smaller values of $\tau_1$ and $\tau_2$, i.e. for larger cut-off frequencies, however, the spike–spike-correlations increase strongly. For e.g. $\tau_1 = 1$ and $\tau_2 = 0.01$, the contribution of spike–spike correlations to the spectral density exceeds the shot-noise contribution.

## 6. Signal-to-noise ratio

For applications, a large signal-to-noise ratio (SNR) of the output might be more important than a large signal intensity. It is by no means clear whether the noise level which optimizes the intensity of the signal-spike in the power spectrum is a good choice for achieving a large SNR.

The starting point for our considerations is Eq. (17), i.e. the splitting of the spectral density into a white shot-noise contribution $\langle r_{cr}(t) \rangle_t$, a sum of sharp $\delta$-peaks (19) $S_\delta(\omega)$ stemming from the periodicity of the correlation for large times, and the contribution $\gamma(\omega)$ from spike–spike correlations. Neglecting the contribution from spike–spike correlations, justified for $\Omega^2 \tau_1 \tau_2 > 1$, the noise background is simply given by the time averaged threshold crossing rate which is obtained from (9) by an integration. The approximated SNR, given by

$$\mathrm{SNR} = \frac{4\pi |c_1|^2}{\langle r_{cr} \rangle_t}, \tag{27}$$

is shown as a function of the variance $\bar{\sigma}^2 = \sigma^2/b^2$ of the noise in Fig. 4. It shows – similar to the signal intensity – a resonance-like curve. The noise level $\bar{\sigma}^2$, which maximizes the SNR, is lower than the noise level which maximizes the signal intensity (see Fig. 1a).

For amplitudes of the input signal larger than the threshold ($\bar{A} > 1$), the SNR decreases – in contrast to the signal amplitude – monotonically for increasing noise strength.

For a weak input signal, the approximations for small $\bar{A}$ and the neglect of pair correlations in the noise background allow one to derive an explicit expression for the SNR of the spike train, i.e.

$$\mathrm{SNR}_{out}(\epsilon \to 0) = \frac{\bar{A}^2}{2\bar{\sigma}^4 \sqrt{\tau_1 \tau_2}} \exp(-1/2\bar{\sigma}^2). \tag{28}$$

With the signal-to-noise ratio of the input

$$\mathrm{SNR}_{in}(\epsilon \to 0) = \frac{\pi \bar{A}^2}{(\tau_1 + \tau_2)\bar{\sigma}^2}, \tag{29}$$

the ratio of the SNR of the output and that of the input is given by

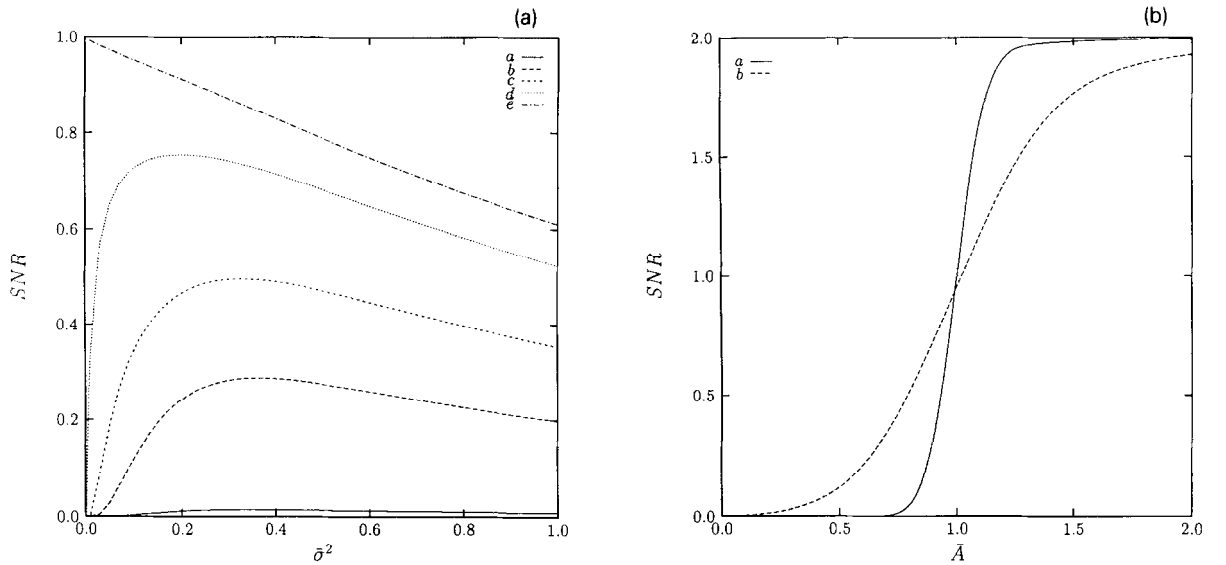


Fig. 4. (a) SNR as a function of the noise level for $\bar{A} = 0.1$ (a), $\bar{A} = 0.5$ (b), $\bar{A} = 0.7$ (c), $\bar{A} = 0.9$ (d), and $\bar{A} = 1.0$ (e) at $\tau_1 = 2, \tau_2 = 1$ and $\epsilon = \sqrt{\Omega^2 \tau_1 \tau_2} = \sqrt{2}$. (b) SNR as a function of the signal amplitude $\bar{A}$ for $\sigma^2 = 0.01$ (a) and $\sigma^2 = 0.1$ (b) at $\tau_1 = 2, \tau_2 = 1$ and $\epsilon = \sqrt{\Omega^2 \tau_1 \tau_2} = \sqrt{2}$. The SNRs shown in (a) and (b) have been obtained by neglecting spike–spike correlations.

$$\frac{\mathrm{SNR}_{\mathrm{out}}}{\mathrm{SNR}_{\mathrm{in}}}(\epsilon \to 0) = \frac{1}{2\pi\bar{\sigma}^2} \frac{\tau_1 + \tau_2}{\sqrt{\tau_1 \tau_2}} \exp(-1/2\bar{\sigma}^2). \tag{30}$$

For sufficiently small $\tau_1$ or $\tau_2$ Eq. (30) would imply a larger SNR of the output than the input for some values of the noise strength. At this point, however, it becomes important to consider the contribution of the spike–spike correlations to the spectral density. In Fig. 5, we compare the signal-to-noise ratio of the output including the contribution from spike–spike correlation with the SNR obtained by neglecting the spike–spike correlations. It is interesting to note that the inclusion of spike–spike correlations can result in an increase or decrease of the SNR. The SNR of the output, however, remained smaller than the SNR of the input for all parameter values we have studied (for bistable systems, see the discussion on this issue in Ref. [10]).

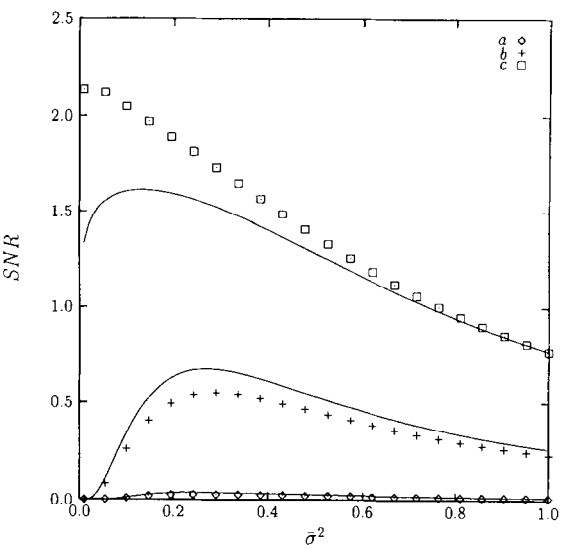


Fig. 5. The SNR obtained by neglecting the spike–spike correlations (solid lines) are compared to the exact SNRs for $\bar{A} = 0.1$ (a), $\bar{A} = 0.5$ (b), $\bar{A} = 1$ (c) at $\tau_1 = 0.9, \tau_2 = 0.1$ and $\epsilon = \sqrt{\Omega^2 \tau_1 \tau_2} = 0.3$.

## 7. Optimal design of threshold devices

In this section, we consider the question how to tune the parameters of the threshold system to achieve optimal performance, whereas performance is measured by the signal intensity at the output, or alternatively,

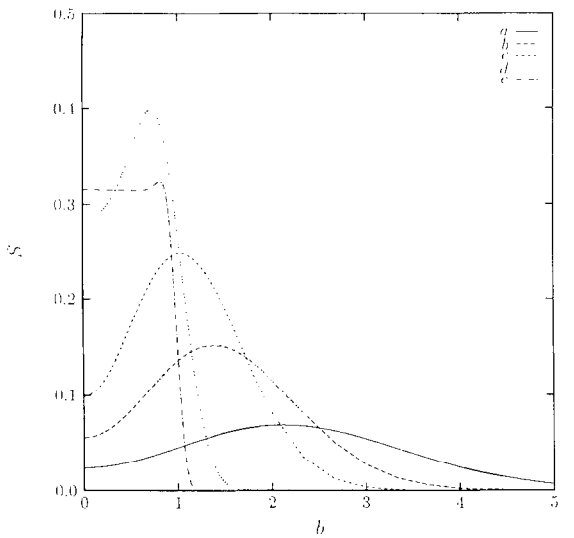


Fig. 6. Signal intensity of the output as a function of the design-parameter (threshold) $b/A$ for $\bar{A}^2/\bar{\sigma}^2 = 0.1$ (a), $\bar{A}^2/\bar{\sigma}^2 = 0.5$ (b), $\bar{A}^2/\bar{\sigma}^2 = 1$ (c), $\bar{A}^2/\bar{\sigma}^2 = 10$ (d), $\bar{A}^2/\bar{\sigma}^2 = 100$ (e) at $\tau_1 = 0.9, \tau_2 = 0.1$ and $\epsilon = \sqrt{\Omega^2\tau_1\tau_2} = 0.3$.

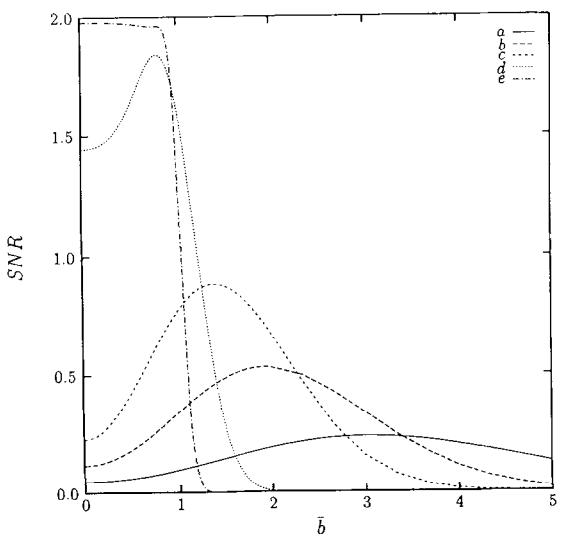


Fig. 7. SNR of the output as a function of the design-parameter (threshold) $b/A$ for $\bar{A}^2/\bar{\sigma}^2 = 0.1$ (a), $\bar{A}^2/\bar{\sigma}^2 = 0.5$ (b), $\bar{A}^2/\bar{\sigma}^2 = 1$ (c), $\bar{A}^2/\bar{\sigma}^2 = 10$ (d), $\bar{A}^2/\bar{\sigma}^2 = 100$ (e) at $\tau_1 = 0.9, \tau_2 = 0.1$ and $\epsilon = \sqrt{\Omega^2\tau_1\tau_2} = 0.3$.

by the SNR.

In the case of a fixed threshold $b$ and variable noise, the signal intensity of the output has been plotted in Fig. 1a as a function of the noise-level. For a large range of given amplitudes of the input signal $A$, there is a finite noise level which optimizes the signal intensity of the output. The SNR can be maximized for signals below threshold at a finite, but different noise level (see Fig. 4a).

A more realistic situation is that the input signal and noise (signal/noise ratio) is a given quantity and all that can be tuned is the threshold $b$, the design-parameter. Characterizing the input by $\bar{A}^2/\bar{\sigma}^2$, being proportional to its SNR (29), we show the signal intensity as a function of the threshold $b$ in Fig. 6. For a large SNR of the input, the best performance is obtained at a threshold value $b$ smaller than the amplitude of the input signal $A$; once this condition is fulfilled the performance is approximately constant. This result is not very surprising and reflects the conventional design strategy, i.e. the threshold has to be small enough that the signal can cross and cause spiking. It is far more surprising that this design-strategy is not a very good one for input signals having a small SNR. Fig. 6 shows that in such cases it is better to choose a threshold $b$ *above* the amplitude of the input signal $A$. This result can be understood as follows:

For a very large threshold, spiking is a rare event and thus the signal intensity of the output is small. For decreasing, but still large thresholds ($b \gg A$), the noise induced spiking rate will increase but will be synchronized with the input signal, yielding increasing signal intensities. For further decreasing values of $b$, the spike rate will further increase, but many spikes are spontaneous and not correlated with the input signal, yielding eventually a decrease of the signal intensities in the output.

In Fig. 7, we show the SNR of the output as a function of the threshold $b$ for various SNRs of the signal input. Similar to the signal intensity, the SNR also peaks for input signals with a low SNR at thresholds larger than the amplitude of the input signal.

The consequence of these results is of potential importance for technical applications. Given the environmental conditions, i.e. a typical environmental noise and a typical size of the input signal to be detected, there is an optimal value of the threshold which *is determined* by the environmental conditions. In Ref.

[11], we suggest as an application a two-dimensional array of threshold elements as a speed-selective detector for moving targets which can be tuned to the environmental conditions.

## Acknowledgement

I would like to thank the Deutsche Forschungsgmeinschaft for financial support within the Heisenberg program.

## Appendix A

In this Appendix, we give a brief discussion on the statistics of the threshold crossing times of a spiking threshold device introduced in Section 1, based on the theory of random point processes (for a comprehensive introduction, see Ref. [12]).

The number of threshold crossings in the interval $[0,t]$ is given by

$$n(t) = \int_0^t |\dot{x}|(t')\delta(x(t'))\Theta(\dot{x}(t')) \tag{31}$$

The probability of finding $n$ crossings given by

$$p(n) = \langle \delta_{n(t),n} \rangle \tag{32}$$

yields the characteristic function [13]

$$I(k) = \langle e^{ikn(t)} \rangle = \left\langle \exp\left( ik \int_0^t dt' \, |\dot{x}(t')|\Theta(\dot{x}(t')) \times \delta(x(t') - b) \right) \right\rangle. \tag{33}$$

The moments $\langle n(t) \rangle$ and $\langle n^2(t) \rangle$, i.e. the mean number of crossings and the fluctuations of this number, are obtained by the first and second derivative of the characteristic function $I(t)$,

$$\langle n(t) \rangle = -iI'(0) = \int_0^t dt' \int_0^\infty dv \, P(b,v,t'), \tag{34}$$

$$\langle n^2(t) \rangle = -I''(0) = \int_0^t dt' \int_0^t dt'' \, K_2(t',t''), \tag{35}$$

with

$$K_2(t,t') = \int_0^\infty dv \int_0^\infty dv' \, vv' \times P(b,v,t|b,v',t')P(b,v',t'). \tag{36}$$

$P(x,v,t)$ and $P(x,v,t|x',v',t')$ are the single event and transition probability densities, respectively, given in Section 5. Using the probability densities $f_m(t_1,t_2,...,t_m)$ defined via the moments $\langle n^m(t) \rangle$ [12],

$$\langle n(t) \rangle = \int_0^t f_1(t') \, dt',$$

$$\langle n^2(t) \rangle = \langle n(t) \rangle + \int_0^t dt' \int_0^t dt'' \, f_2(t',t''), \tag{37}$$

we find

$$f_1(t) = \langle \dot{n}(t) \rangle = \int_0^\infty dv \, vP(b,v,t),$$

$$f_2(t,t') = f_1(t)\delta(t-t') - K_2(t,t'), \tag{38}$$

where $f_n(t_1,t_2,...,t_m)$ denote the probability of having one crossing event in each of the intervals $[t_1, t_1 + dt_1], [t_2, t_2 + dt_2], ..., [t_m, t_m + dt_m]$, regardless of how many crossings have occurred outside the interval $[t_1, t_m]$.

The covariance function $k_2(t,t') = K_2(t,t') - f_1(t)f_1(t')$ can then be expressed as the sum of a $\delta$-contribution (white shot noise) and a spike–spike correlation function (in the literature, the term pair-correlation function is more common), i.e. [7]

$$k_2(t,t') = \langle \dot{n}(t) \rangle \delta(t-t') + g_2(t,t'),$$

$$g_2(t,t') = f_2(t,t') - f_1(t)f_1(t'). \tag{39}$$

For a Poissonian process (white shot noise), the spike–spike correlation function vanishes identically.

## References


[1] K. Wiesenfeld, D. Pierson, E. Pentazelou, C. Dames and F. Moss, Phys. Rev. Lett. 72 (1994) 2125.

[2] Z. Gingl, L. Kiss and F. Moss, Europhys. Lett. 29 (1995) 191.

[3] K. Wiesenfeld and F. Moss, Nature 373 (1995) 33.

[4] R. Benzi, A. Sutera and A. Vulpiani, J. Phys. A 14 (1981) L453;
C. Nicholis, Tellus 34 (1982) 1;
B. McNamara and K. Wiesenfeld, Phys. Rev. A 39 (1989) 4854;
L. Gammaitoni, F. Marchesoni, E. Manichella-Saetta and S. Santucci, Phys. Rev. Lett. 62 (1989) 349;
Hu Gang, G. Nicolis and C. Nicolis, Phys. Rev. A 42 (1990) 2030;
M.I. Dykman, R. Mannella, P.V.E. McClintock and N.G. Stocks, Phys. Rev. Lett. 65 (1990) 2606;
F. Moss, Ber. Bunsenges. Phys. Chem. 95 (1991) 303;
P. Jung and P. Hanggi, Phys. Rev. A 44 (1991) 8032;
F. Moss, A. Bulsara and M. Shlesinger, eds., J. Stat. Phys. 70 (1993) 1–514;
A.R. Bulsara, G. Schmera, Phys. Rev. A 47 (1993) 3734;
R.F. Fox and Yan-nan Lu, Phys. Rev. E 48 (1993) 3390;
J.K. Douglas, L. Wilkens, E. Pentazelou and F. Moss, Nature 365 (1993).

[5] P. Jung, Phys. Rep. 234 (1993) 175.

[6] F. Moss, in: Frontiers in applied mathematics, ed. G. Weiss (SIAM, Philadelphia, 1994).

[7] R.L. Stratonovich, Theory of random noise, Vols. I and II (Gordon and Breach, New York, 1964).

[8] P. Jung and P. Hanggi, Phys. Rev. A 41 (1990) 2977.

[9] P. Jung, Phys. Rev. E 50 (1994) 2513.

[10] M.E. Inchiosa and A.R. Bulsara, Phys. Rev. E 52 (1995) 327.

[11] G. Mayer-Kress and P. Jung, in preparation.

[12] N.G. van Kampen, Stochastic processes in physics and chemistry (North-Holland, Amsterdam, 1984).

[13] E. Pollak and P. Talkner, Phys. Rev. E 51 (1995) 1868.